© 2019. Published by The Company of Biologists Ltd | Journal of Cell Science (2019) 132, jcs221663. doi:10.1242/jcs.221663

RESEARCH ARTICLE

Deubiquitylase USP9X maintains centriolar satellite integrity by stabilizing pericentriolar material 1 protein

Ke-Jun Han[1], Zhiping Wu[2], Chad G. Pearson[3], Junmin Peng[2], Kunhua Song[4] and Chang-Wei Liu[1,*]

ABSTRACT

Centriolar satellites are small cytoplasmic granules that play important roles in regulating the formation of centrosomes and primary cilia. Ubiquitylation of satellite proteins, including the core satellite scaffold protein pericentriolar material 1 (PCM1), regulates centriolar satellite integrity. Currently, deubiquitylases that control centriolar satellite integrity have not been identified. In this study, we find that the deubiquitylase USP9X binds PCM1, and antagonizes PCM1 ubiquitylation to protect it from proteasomal degradation. Knockdown of USP9X in human cell lines reduces PCM1 protein levels, disrupts centriolar satellite particles and causes localization of satellite proteins, such as CEP290, to centrosomes. Interestingly, knockdown of mindbomb 1 (MIB1), a ubiquitin ligase that promotes PCM1 ubiquitylation and degradation, in USP9X-depleted cells largely restores PCM1 protein levels and corrects defects caused by the loss of USP9X. Overall, our study reveals that USP9X is a constituent of centriolar satellites and functions to maintain centriolar satellite integrity by stabilizing PCM1.

KEY WORDS: Deubiquitylase, Deubiquitylation, USP9X, Centriolar satellites, PCM1

INTRODUCTION

The centriolar satellite, centrosome and primary cilium network plays an important role in development by mediating signal transduction (Chavali et al., 2014; Conkar et al., 2017; Hori and Toda, 2017; Kurtulmus et al., 2016; Tollenaere et al., 2015). Centriolar satellites are small cytoplasmic granules that cluster in the vicinity of centrosomes (Bärenz et al., 2011; Hori et al., 2015; Hori and Toda, 2017; Tollenaere et al., 2015). Centriolar satellites contain more than 100 proteins (Chavali et al., 2014; Hori and Toda, 2017). One major proposed function of centriolar satellites is to transport proteins from the cytoplasm into centrosomes or primary cilia to regulate their assembly (Hori et al., 2015; Hori and Toda, 2017). In addition, centriolar satellites could be involved in regulating stress response and autophagy (Joachim et al., 2017; Shearer et al., 2016). Mutations in genes encoding centriolar satellite proteins, including CEP290, OFD1 and BBS4, cause ciliopathies that are genetic disorders causing kidney diseases, blindness, developmental retardation and neurological problems (Coene et al., 2009; Ferrante et al., 2009; Frank et al., 2008; Helou et al., 2007; Katsanis et al., 2001; Lopes et al., 2011; Perrault et al., 2007; Valente et al., 2006). Currently, mutations in a large body of genes in the centriolar satellite, centrosome and primary cilium network have been identified to cause ciliopathies.

Pericentriolar material 1 (PCM1) is a structural scaffold protein and a cellular marker of centriolar satellites (Hori and Toda, 2017; Tollenaere et al., 2015). PCM1 recruits proteins, including CEP290, OFD1, BBS4 and CEP131, to form the structural platform for assembly of centriolar satellites. Depletion of PCM1 disrupts centriolar satellites and causes mislocalization of centrosomal and satellite proteins (Dammermann and Merdes, 2002; Kim et al., 2008; Wang et al., 2016). Post-translational modification of PCM1 was found to regulate centriolar satellite integrity. Polo-like kinase 4 (PLK4) binds and phosphorylates PCM1 at serine 372, which mediates PCM1 dimerization and interaction with other satellite proteins such as BBS4 and CEP290. Depletion of PLK4 leads to dispersion of centriolar satellite particles (Hori et al., 2016; Hori and Toda, 2017). PCM1 can also be phosphorylated by other cell cycle-related kinases, including CDK1 and PLK1 (Hori and Toda, 2017; Olsen et al., 2010; Santamaria et al., 2011). It is speculated that phosphorylation of PCM1 by different kinases may regulate, at least in part, the cell cycle-dependent centriolar satellite remodeling (Hori et al., 2016; Hori and Toda, 2017; Zhang et al., 2017). The E3 ubiquitin ligase mindbomb 1 (MIB1) localizes to centriolar satellites by binding to PCM1 (Wang et al., 2016). MIB1 catalyzes PCM1 polyubiquitylation to promote proteasomal degradation (Wang et al., 2016), thereby functioning as a destabilizer of centriolar satellites. Another study found that MIB1 mediates monoubiquitylation of PCM1, CEP131 and CEP290, which was proposed to maintain centriolar satellite structures under non-stressed conditions, although the underlying mechanism is not known (Villumsen et al., 2013).

USP9X is a large deubiquitylase (~290 kDa) that deubiquitylates substrates conjugated with monoubiquitin and/or polyubiquitin chains (Al-Hakim et al., 2008; Dupont et al., 2009; Schwickart et al., 2010). Loss-of-function mutations in *USP9X* cause female-specific syndromes, including intellectual disability and defects in neural development, typical phenotypes seen in ciliopathies (Homan et al., 2014; Paemka et al., 2015; Reijnders et al., 2016). In this regard, USP9X was found to localize along the ciliary axoneme in fibroblasts, but knockdown of USP9X has no effect on ciliogenesis (Reijnders et al., 2016). In another study, IQCB1 was found to recruit USP9X into centrosomes, where USP9X protects IQCB1 from ubiquitylation and degradation, which promotes ciliogenesis in human retinal pigment epithelium (RPE) cells (Das et al., 2017). In addition, two recent studies have found that USP9X regulates centrosome duplication (Li et al., 2017; Wang et al., 2017). Wang et al. (2017) showed that USP9X colocalizes with PCM1 and CEP55 in centrosomes. USP9X controls the protein

[1]Department of Biochemistry and Molecular Genetics, University of Colorado Anschutz Medical Campus, Aurora, CO 80045, USA. [2]Departments of Structural Biology and Developmental Neurobiology, St. Jude Proteomics Facility, St. Jude Children's Research Hospital, Memphis, TN 38105, USA. [3]Department of Cell and Developmental Biology, University of Colorado Anschutz Medical Campus, Aurora, CO 80045, USA. [4]Division of Cardiology, Department of Medicine, University of Colorado Anschutz Medical Campus, Aurora, CO 80045, USA.

*Author for correspondence (Changwei.Liu@ucdenver.edu)

C.-W.L., 0000-0002-6449-384X

Received 18 June 2018; Accepted 19 December 2018

Journal of Cell Science (2019) 132, jcs221663. doi:10.1242/jcs.221663

abundances of PCM1 and CEP55, which could contribute to the requirement of USP9X in centrosome duplication. Li et al. (2017) found that USP9X colocalizes with CEP131 in centrosomes. USP9X binds and deubiquitylates CEP131 to antagonize proteasomal degradation, which could also contribute to the requirement of USP9X in centrosome duplication. Intriguingly, both PCM1 and CEP131 are also key centriolar satellite proteins. Whether USP9X is a centriolar satellite protein and its role in regulating centriolar satellite functions have not been investigated. In this study, our results reveal that USP9X deubiquitylates PCM1 to protect it from proteasomal degradation, by which USP9X stabilizes PCM1 and is required for maintaining centriolar satellite integrity.

RESULTS

USP9X colocalizes with PCM1 in centriolar satellites

In a previous study, we identified survival motor neuron (SMN) protein as a substrate of USP9X-mediated deubiquitylation. USP9X stabilizes the SMN complex and plays an important role in regulating Cajal body formation in the nucleus (Han et al., 2012). In that study, we performed a proteomics study to identify USP9X-interacting proteins; several proteins in the centriolar satellite, centrosome and primary cilium network, including CEP290, IQCB1, ATXN10 and CEP170, were identified with trypsinization-derived peptides (Han et al., 2012) (Fig. S1 and data not shown). We initiated our current study by investigating the interaction between USP9X and CEP290, because CEP290 is an important protein in the centriolar satellite, centrosome and primary cilium network. First, we found that endogenous USP9X interacted with CEP290 in 293T cells in a co-immunoprecipitation assay (Fig. 1A). Second, immunostaining showed that CEP290 existed as cytoplasmic foci, and USP9X primarily localizes in the cytoplasm of HeLa cells (Fig. 1B), 293T and HCT116 cells (data not shown). Remarkably, USP9X colocalized with CEP290 in foci in these cell lines. Lastly, using FLAG-tagged USP9X deletion mutants expressing USP9X(1–966), USP9X(967–1537), USP9X(1531–1971) or USP9X(1971–2554), immunoprecipitation assays revealed that the N-terminal USP9X fragment, USP9X(1–966), interacted with endogenous CEP290 (Fig. 1C,D). Collectively, these results demonstrate that USP9X and CEP290 form a protein complex in the cell, requiring the N-terminal region of USP9X.

CEP290 resides in centriolar satellites, centrosomes and primary cilia (Coppieters et al., 2010; Drivas and Bennett, 2014; Kim et al., 2008). To identify subcellular structures in which USP9X colocalizes with CEP290, we colocalized USP9X with a centrosomal marker, γ-tubulin, and a centriolar satellite marker, PCM1. USP9X primarily localized within the cytoplasm (Fig. 1B), but a small population of USP9X formed foci partially colocalizing with and largely surrounding γ-tubulin foci (Fig. 1E,F). Thus, the majority of foci-like USP9X surrounds centrosomes. In contrast, foci-like USP9X primarily colocalized with the centriolar satellite component PCM1 (Fig. 1E,F). PCM1 can dynamically traffic to centrosomes (Dammermann and Merdes, 2002; Kim et al., 2008; Lopes et al., 2011). Co-staining of PCM1 with γ-tubulin showed that PCM1 foci largely surrounded γ-tubulin with partial colocalization (Fig. 1E,F). These results indicate that the majority of PCM1 foci in HeLa and HCT116 are centriolar satellites, in which USP9X colocalizes.

The clustering of centriolar satellites around centrosomes depends upon microtubule-based transport (Dammermann and Merdes, 2002; Hori and Toda, 2017). Disrupting the microtubule network impairs centriolar satellites, but not centrosomes (Hori and

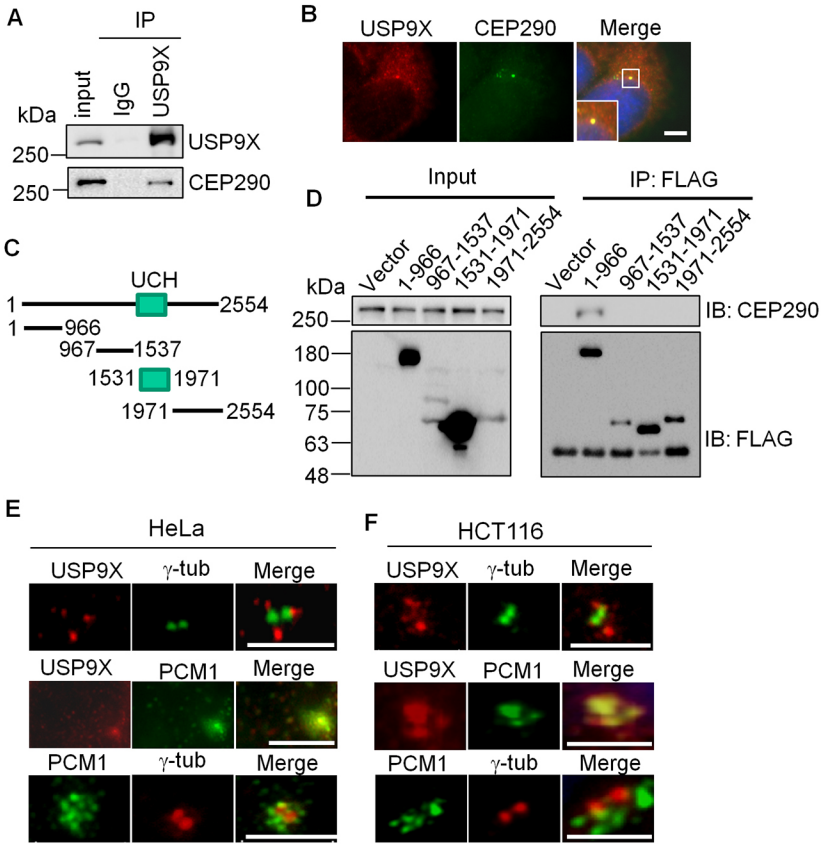

Fig. 1. USP9X resides in centriolar satellites.
(A) Endogenous USP9X in 293T cells was immunoprecipitated using an anti-USP9X antibody, followed by immunoblotting of CEP290 and USP9X. (B) HeLa cells were co-immunostained with antibodies recognizing USP9X (red) and CEP290 (green). For better visualization, a selected area (white outline box) was magnified and is shown in the inset. (C) Schematic illustration of USP9X deletion mutants. (D) Empty pRK7 vector or a FLAG-tagged USP9X deletion mutant was transfected into 293T cells. Expressed proteins were immunoprecipitated with an anti-FLAG antibody, followed by immunoblotting of FLAG and CEP290. (E) Co-immunostaining of USP9X with γ-tubulin or PCM1, and co-immunostaining of PCM1 with γ-tubulin, in HeLa cells. For better visualization, only the centrosome and centriolar satellite areas of one cell are shown. (F) Similar immunostaining assays as shown in E using HCT116 cells. All experiments were repeated at least three times. Scale bars: 5 µm.

Journal of Cell Science (2019) 132, jcs221663. doi:10.1242/jcs.221663

Toda, 2017; Kim et al., 2008). We therefore examined whether PCM1-positive large foci are affected by microtubule depolymerization. Indeed, nocodazole-mediated microtubule depolymerization caused dispersion of PCM1 (Fig. S2), further supporting that the PCM1-positive foci in which USP9X colocalizes are centriolar satellites.

The middle region of PCM1 interacts with the C-terminal region of USP9X

USP9X was found to bind PCM1 in co-immunoprecipitation assays (Li et al., 2017; Wang et al., 2017). Consistent with previous reports, endogenous PCM1 and USP9X in HeLa cells formed a protein complex in a co-immunoprecipitation assay (Fig. 2A). Knockdown of CEP290 had no effect on the protein levels of USP9X and PCM1, as well as their interaction (Fig. 2B), indicating that CEP290 does not mediate the PCM1 and USP9X interaction. Next, we generated deletion mutants of the PCM1 isoform 14 (1859 amino acids) (Fig. 2C). Expressed PCM1(1–1300) and PCM1(851–1859), but not PCM1(1–400), pulled down endogenous USP9X in co-immunoprecipitation assays. PCM1(1–850) and PCM1(1301–1859) weakly interacted with USP9X (Fig. 2D). These results indicate that the middle region of PCM1, mainly between 851 and 1300 amino acids, interacts with USP9X. We then generated a PCM1 fragment expressing Myc-tagged PCM1(851–1300). Co-immunoprecipitation assays revealed that Myc-PCM1(851–1300) interacted with FLAG-USP9X(1971–2554) when co-expressed in 293T cells (Fig. 2E). The USP9X(967–1537) fragment was expressed at low levels. We were unable to obtain high-purity recombinant GST-PCM1 or GST-PCM1(851–1300), which restrained us from assessing whether PCM1 directly binds USP9X using GST pulldown assays. Nevertheless, these results indicate that USP9X forms a protein complex with PCM1 in the cell, requiring the middle region of PCM1 and the C-terminal region of USP9X.

USP9X deubiquitylates PCM1 and protects it from proteasomal degradation

siRNA-mediated depletion of USP9X reduces PCM1 protein levels (Li et al., 2017; Wang et al., 2017). We confirmed that stable knockdown of USP9X using two distinct shRNA constructs in HeLa or HCT116 cells caused significant reduction of PCM1 protein levels (Fig. 3A). Interestingly, CEP290 protein levels were reduced in HCT116 cells, but not in HeLa cells, upon depletion of USP9X, indicating a cell type-specific effect (Fig. 3A). In contrast, knockdown of another deubiquitylase, USP7, had no effect on protein levels of PCM1 or CEP290 (Fig. 3B). The proteasome inhibitor MG132, but not the lysosome inhibitor bafilomycin A1, blunted the PCM1 protein level difference between control and USP9X knockdown cells (Fig. 3C). Lower levels of PCM1 protein in MG132-treated cells than those in dimethyl sulfoxide (DMSO)- or bafilomycin-treated cells were likely due to cell death, as judged by low α-tubulin (a loading control) protein levels in these samples.

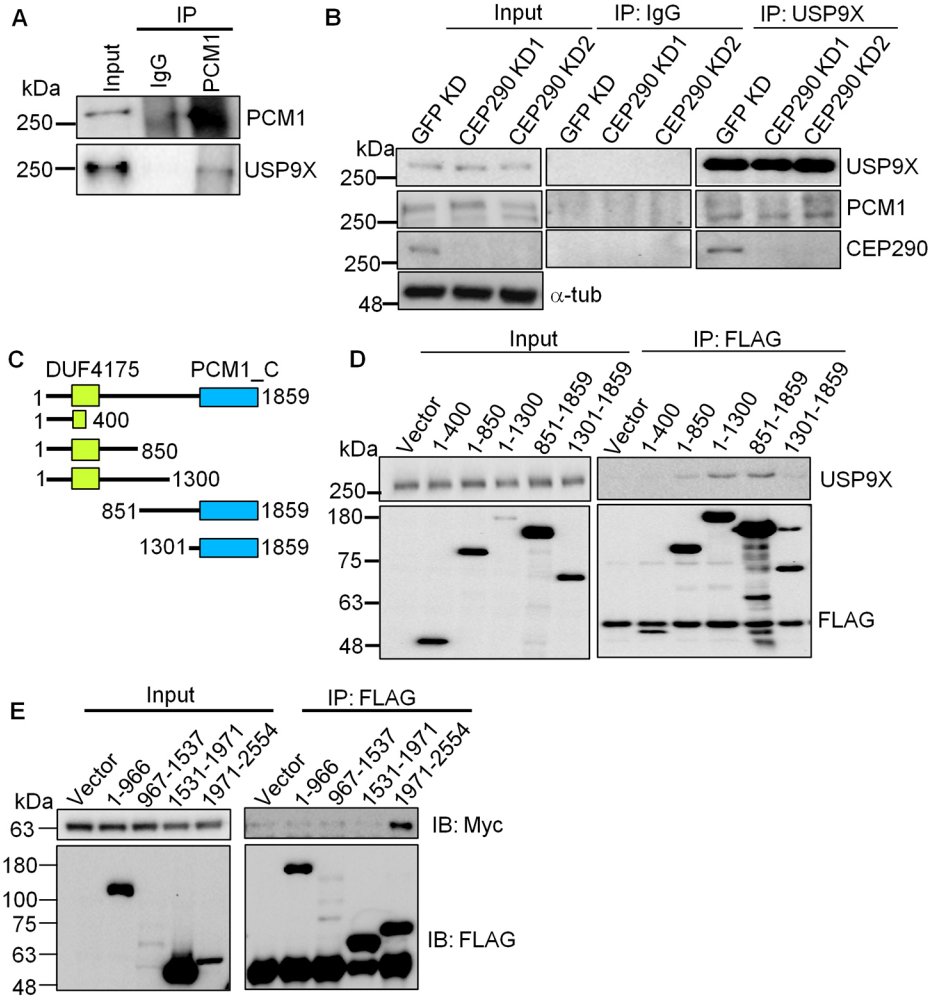

Fig. 2. The middle region of PCM1 interacts with the C-terminal region of USP9X. (A) Endogenous PCM1 in HeLa cells was immunoprecipitated using an anti-PCM1 antibody, followed by immunoblotting of PCM1 and USP9X. (B) CEP290 in HeLa cells was knocked down using two distinct shRNA constructs. GFP (control) or CEP290 knockdown cell lysates were used for immunoprecipitation of endogenous USP9X, followed by immunoblotting assays. (C) Schematic illustration of PCM1 deletion mutants. (D) Empty pRK7 vector or a FLAG-tagged PCM1 deletion mutant was transfected in 293T cells. Expressed proteins were immunoprecipitated with an anti-FLAG antibody, followed by immunoblotting of FLAG and USP9X. (E) Myc-PCM1(851–1300) was co-transfected with an empty pRK7 vector or a FLAG-tagged USP9X deletion mutant in 293T cells. Expressed USP9X proteins were immunoprecipitated with an anti-FLAG antibody, followed by immunoblotting of FLAG and Myc. All experiments were repeated at least twice.

Journal of Cell Science (2019) 132, jcs221663. doi:10.1242/jcs.221663

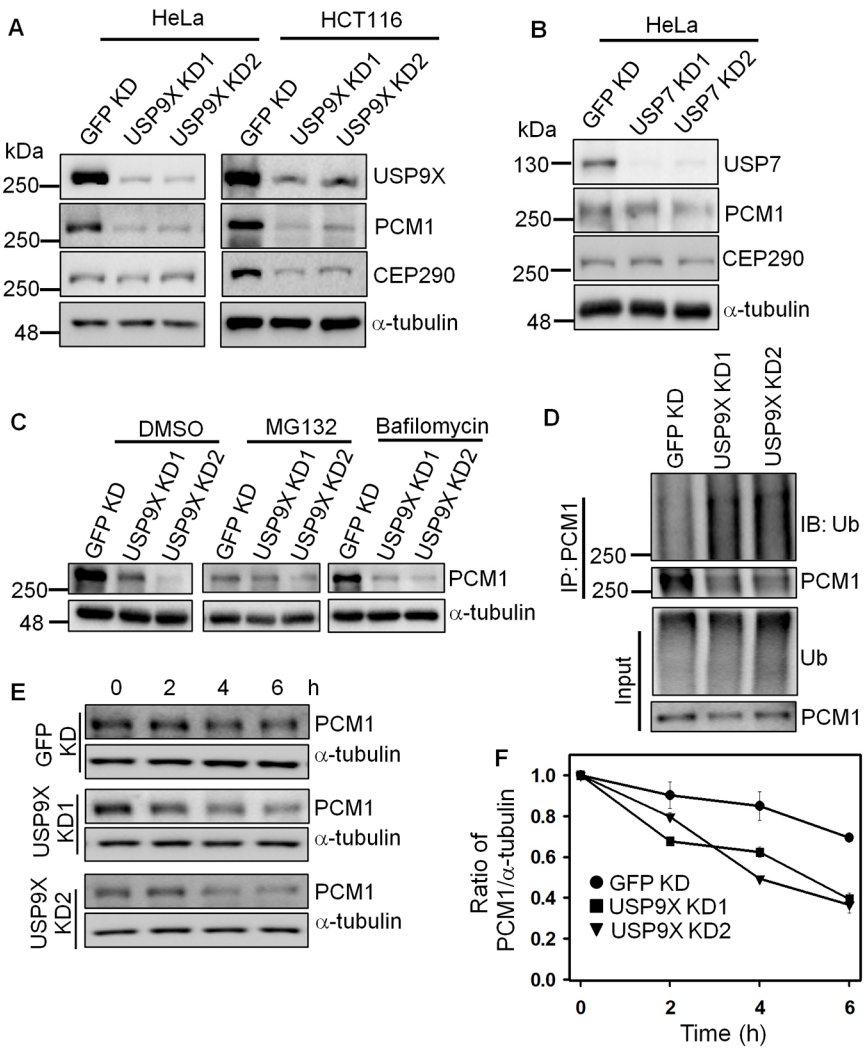

Fig. 3. USP9X antagonizes ubiquitin-dependent proteasomal degradation of PCM1. (A) Whole-cell lysates of GFP or USP9X knockdown HeLa or HCT116 cells were applied for immunoblotting of USP9X, CEP290, PCM1 and α-tubulin. (B) USP7 was knocked down using two distinct shRNA constructs in HeLa cells. Cell lysates were applied for immunoblotting of USP7, PCM1, CEP290 and α-tubulin. (C) GFP or USP9X knockdown HeLa cells were treated with DMSO, MG132 (10 µM) or bafilomycin (100 nM) for 16 h. Cell lysates were immunoblotted with an anti-PCM1 or anti-α-tubulin antibody. (D) Cell lysates of GFP or USP9X knockdown HeLa cells were immunoprecipitated using an anti-PCM1 antibody under a denaturing condition, followed by immunoblotting of ubiquitin (Ub) and PCM1. (E) GFP or USP9X knockdown HeLa cells were treated with 100 µg/ml cycloheximide (CHX) and then harvested at each indicated time point. Whole-cell lysates were applied for immunoblotting of α-tubulin and PCM1. No CHX treatment for time zero samples. (F) The PCM1/α-tubulin ratios in the experiment shown in E were quantitated by densitometry. Each ratio at time zero was referenced as 1. Error bars represent s.d. of three independent experiments. Experiments in A–D were repeated at least twice.

Thus, USP9X knockdown may promote proteasomal degradation of PCM1.

Next, we asked whether PCM1 is a substrate of USP9X-mediated deubiquitylation. To examine this, endogenous PCM1 in USP9X or control knockdown cell lysates were subjected to denaturing immunoprecipitation, which can avoid non-specific binding. Immunoblotting of ubiquitin showed that depletion of USP9X resulted in a substantial elevation of PCM1 ubiquitylation, despite less PCM1 being immunoprecipitated in USP9X knockdown cells than that in GFP knockdown cells (Fig. 3D). Lastly, we examined the protein half-life of endogenous PCM1 in USP9X or control knockdown cells using the cycloheximide-chase assay. Depletion of USP9X using either of the shRNA constructs greatly shortened the protein half-life of PCM1 compared with that of control knockdown cells, when analyzed by immunoblotting assays (Fig. 3E) and densitometric quantification of immunoblots (Fig. 3F). Taken together, these results demonstrate that USP9X stabilizes PCM1 by deubiquitylating PCM1 to protect it from proteasomal degradation.

USP9X is required for centriolar satellite integrity

PCM1 is a core structural protein of centriolar satellites (Hori and Toda, 2017; Tollenaere et al., 2015). Because USP9X stabilizes PCM1, we predicted USP9X to be a key regulator of centriolar satellite integrity. To assess this prediction, we mixed GFP knockdown cells with USP9X knockdown cells to create two cell populations that express either high or low USP9X protein levels. The mixed cells were co-immunostained with anti-USP9X and anti-PCM1 antibodies to visualize their colocalization. In ∼80% of HeLa cells expressing high USP9X protein levels (marked with a white arrowhead in Fig. 4A and quantification results in B), PCM1 formed large foci that colocalized with USP9X. In contrast, PCM1-positive large foci were only detected in ∼10% of cells expressing low USP9X protein levels (marked with a white arrow in Fig. 4A and quantification results in B). Similar results were also obtained when the same assay was performed by mixing GFP knockdown or USP9X knockdown HCT116 cells (Fig. 4C,D). These results indicate that depletion of USP9X disrupts centriolar satellites.

USP9X is important for localization of CEP290 in centriolar satellites

Centriolar satellites are crucial for the proper localization of some proteins in the centriolar satellite, centrosome and primary cilia network (Kim et al., 2008). CEP290 is found in all three subcellular structures of the network. We next examined whether the localization of CEP290 is affected by USP9X knockdown. In GFP knockdown HeLa cells, CEP290 stained as a few foci that overlapped with PCM1 (Fig. 5A), and surrounded γ-tubulin with partial overlap (Fig. 5B), indicating that the majority of CEP290 resides in centriolar satellites. In striking contrast, in USP9X knockdown HeLa cells, CEP290 stained as two foci that barely

Journal of Cell Science (2019) 132, jcs221663. doi:10.1242/jcs.221663

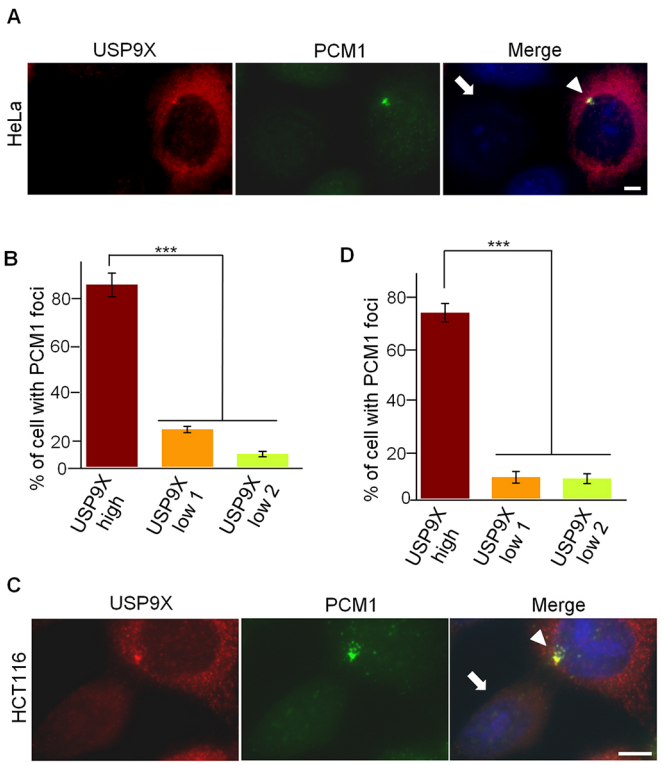

Fig. 4. USP9X is required for maintaining centriolar satellite integrity. (A) GFP or USP9X knockdown HeLa cells were mixed and co-immunostained for USP9X (red) and PCM1 (green). The white arrowhead and arrow point to a GFP or USP9X knockdown cell, respectively. (B) Quantification of cells with PCM1 large foci in USP9X high- or low-expression cells, as judged by immunostaining intensity. Error bars represent s.d. of three areas of cells in a staining experiment. At least 100 cells were counted in each area. ***P<0.001. (C,D) Similar to A and B, except that HCT116 cells were used. All experiments were repeated at least three times. Scale bars: 5 µm.

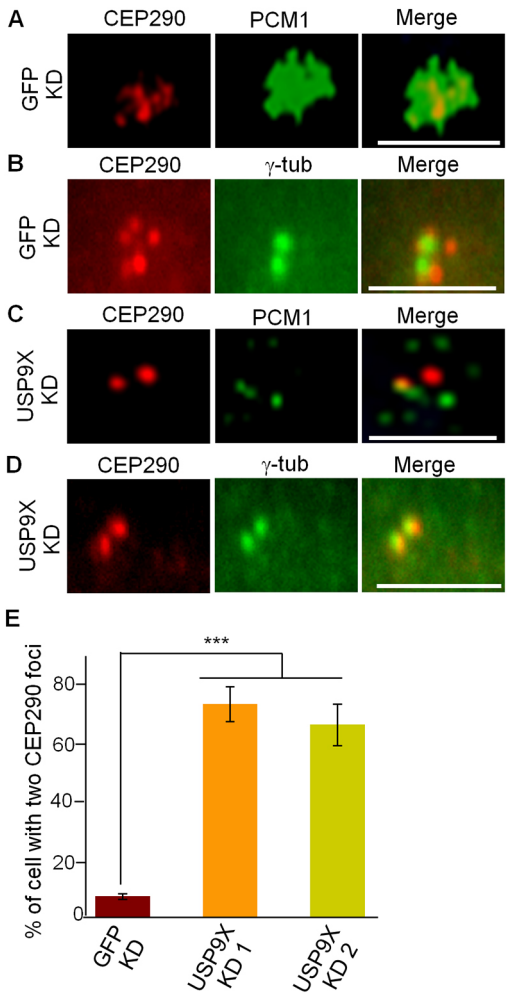

Fig. 5. Depletion of USP9X leads to localization of CEP290 in centrosomes. (A) Co-immunostaining of CEP290 (red) and PCM1 (green) in GFP knockdown HeLa cells. For better visualization, only the centrosome and centriolar satellite areas of a cell in each image are shown. (B) Co-immunostaining of CEP290 (red) and γ-tubulin (green) in GFP knockdown HeLa cells. (C) Co-immunostaining of CEP290 (red) and PCM1 (green) in USP9X knockdown HeLa cells. (D) Co-immunostaining of CEP290 (red) and γ-tubulin (green) in USP9X knockdown HeLa cells. (E) Quantification of cells with two CEP290 foci in GFP or USP9X knockdown cells. At least 100 cells from each cell line were counted each time, and three repeats were performed. ***P<0.001. Scale bars: 5 µm.

co-stained with dispersed PCM1 dots (Fig. 5C), but largely overlapped with γ-tubulin (Fig. 5D). Thus, CEP290 localizes in centrosomes when USP9X is depleted. In quantification, ∼5% GFP knockdown HeLa cells had two CEP290 foci, whereas ∼70% USP9X knockdown cells showed two CEP290 foci (centrosome localization) (Fig. 5E). Overall, these results indicate that loss of USP9X causes localization of CEP290 to centrosomes.

Knockdown of MIB1 corrects defects caused by the loss of USP9X

MIB1 is a ubiquitin ligase that ubiquitylates PCM1 and promotes its proteasomal degradation (Wang et al., 2016). Consistent with the previous study, stable knockdown of MIB1 using two distinct shRNA constructs resulted in a significant accumulation of PCM1 in HeLa cells, despite only ∼50% MIB1 being depleted (Fig. 6A). We therefore expected depletion of MIB1 in USP9X knockdown cells to increase PCM1 protein levels, which, in turn, could rescue defects caused by the loss of USP9X. Indeed, PCM1 protein levels increased from ∼10% in USP9X knockdown cells to ∼50% in USP9X/MIB1 double knockdown cells when referenced to endogenous PCM1 protein levels (comparing lanes 3 and 4 with lane 1 in Fig. 6B). Centriolar satellites re-appeared in USP9X knockdown cells upon MIB1 depletion (marked with a white arrowhead in Fig. 6C). A few USP9X knockdown cells still had high USP9X expression that showed colocalization of USP9X and PCM1 (an example marked with a white arrow in Fig. 6C). Quantification analyses showed that cells with large PCM1 foci increased from ∼6% in USP9X knockdown cells to ∼35% in USP9X and MIB1 double knockdown cells (Fig. 6D). In experiments in which CEP290 and PCM1 were co-immunostained, MIB1 depletion caused re-localization of CEP290 in centriolar satellites (Fig. 6E). Cells with CEP290 and PCM1 colocalization increased from ∼3% in USP9X knockdown cells to ∼36% in USP9X and MIB1 double knockdown cells (Fig. 6F). Collectively, these results indicate that increasing PCM1 protein levels in USP9X knockdown cells corrects defects caused by USP9X depletion. Thus, the role of USP9X in maintaining centriolar satellite integrity is likely due to its ability to stabilize PCM1.

DISCUSSION

In this study, we found that USP9X is required to maintain centriolar satellite integrity. USP9X interacts with and deubiquitylates the centriolar satellite scaffold protein PCM1, and this protects PCM1

Journal of Cell Science (2019) 132, jcs221663. doi:10.1242/jcs.221663

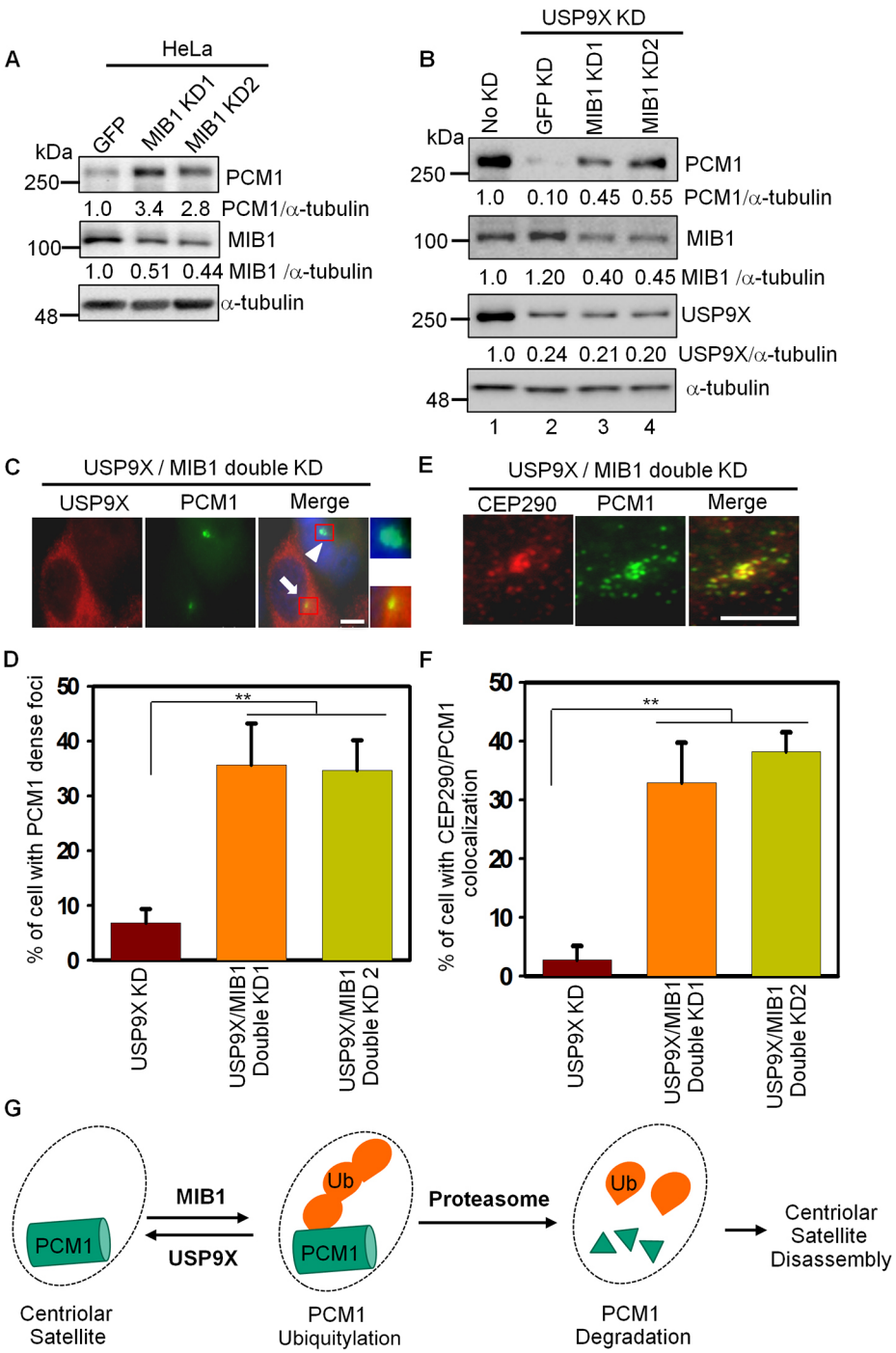

Fig. 6. Knockdown of MIB1 in USP9X-depleted cells corrects defects caused by the loss of USP9X. (A) MIB1 was knocked down by two shRNA constructs in HeLa cells. Whole-cell lysates were applied for immunoblotting of PCM1, MIB1 and α-tubulin. The PCM1/α-tubulin and MIB1/α-tubulin ratios were quantitated by densitometry. (B) USP9X knockdown HeLa cells were used for knockdown of GFP (control) or MIB1 (two shRNAs). Whole-cell lysates were applied for immunoblotting of USP9X, PCM1, MIB1 and α-tubulin. The PCM1/α-tubulin and MIB1/α-tubulin ratios in non-knockdown, USP9X-only knockdown (referred to as GFP knockdown), and USP9X and MIB1 double knockdown HeLa cells were quantitated by densitometry. The ratio in non-knockdown cells was referenced as 1. Experiments in A and B were repeated at least three times. (C) Co-immunostaining of USP9X (red) and PCM1 (green) in USP9X and MIB1 double knockdown HeLa cells. White arrow indicates a USP9X high-expression cell, arrowhead indicates a USP9X knockdown cell. (D) Cells with dense PCM1 foci in USP9X knockdown or USP9X/MIB1 double knockdown were quantitated. (E) Co-immunostaining of CEP290 (red) and PCM1 (green) in USP9X and MIB1 double knockdown HeLa cells. (F) Cells with CEP290/PCM1 colocalization in USP9X knockdown or USP9X/MIB1 double knockdown were quantitated. In D and F, error bars represent s.d. of three areas of cells in a staining experiment. At least 100 cells were counted in each area. $^{**}P<0.01$. (G) A model in which ubiquitylation and deubiquitylation of PCM1 control the centriolar satellite integrity. MIB1-mediated PCM1 ubiquitylation leads to proteasomal degradation of PCM1 and disruption of centriolar satellites. USP9X antagonizes PCM1 ubiquitylation, thereby stabilizing centriolar satellites. Scale bars: 5 µm.

from proteasomal degradation. Knockdown of USP9X decreases PCM1 protein levels, disrupts centriolar satellite particles and localizes CEP290 in centrosomes. Strikingly, depletion of MIB1, a ubiquitin ligase of PCM1, in USP9X knockdown cells increases PCM1 protein levels and corrects defects caused by the loss of USP9X. Thus, USP9X stabilizes PCM1 that is required for maintaining centriolar satellite integrity (Fig. 6G). Recent studies have also found that USP9X regulates centrosome duplication and primary cilium formation (Das et al., 2017; Li et al., 2017; Wang et al., 2017). Altogether, USP9X is an important regulator of the centriolar satellite, centrosome and primary cilium network.

USP9X is a highly conserved and multifunctional deubiquitylase (Murtaza et al., 2015). USP9X primarily localizes in the cytoplasm, but it was also found in cytoplasmic vesicles, Golgi complex, mitochondria and the nucleus (Murray et al., 2004; Murtaza et al., 2015; Schwickart et al., 2010). Recent studies revealed that USP9X localizes in centrosomes by interacting with centrosomal proteins, including IQCB1 (Das et al., 2017), CEP131 (Li et al., 2017) and PCM1 (Li et al., 2017; Wang et al., 2017), through which USP9X regulates centrosome duplication and primary cilia formation. In our study, we observed that USP9X colocalizes with the centrosomal marker γ-tubulin in 293T cells, but sparsely overlaps with γ-tubulin staining in HeLa and HCT116 cells. In contrast, in all examined cell types, USP9X colocalizes with the centriolar satellite marker PCM1, indicating that USP9X is a centriolar satellite protein. A recent study has found that an overexpressed N-terminal region

Journal of Cell Science (2019) 132, jcs221663. doi:10.1242/jcs.221663

of USP9X can pull down endogenous PCM1 (Wang et al., 2017). In our assay, the N-terminal USP9X(1–966) was expressed well, but could not immunoprecipitate any examined PCM1 fragments. Instead, we identified that USP9X(1971–2554), a C-terminal fragment, interacts with the middle region of PCM1, PCM1(850–1300). Formation of a protein complex between USP9X and PCM1 (via a direct or an indirect interaction), and the requirement of USP9X in maintaining centriolar satellite integrity, suggest that USP9X is a bona fide constituent of centriolar satellites.

A few centriolar satellite and centrosomal proteins are substrates for ubiquitylation, including PCM1, CEP290, CEP131 and KIAA0586 (Li et al., 2017; Wang et al., 2016). Knockdown of USP9X could reduce levels of these proteins in cells (Wang et al., 2017). For PCM1, we provided further evidence that USP9X deubiquitylates PCM1, and that depletion of USP9X shortens the protein half-life of PCM1. Thus, USP9X stabilizes PCM1 at the post-translational level by deubiquitylation of PCM1 to prevent proteasomal degradation. Functionally, defects caused by the loss of USP9X are similar to those that have been observed through the loss of PCM1 (Wang et al., 2016), including disruption of centriolar satellite particles and localization of satellite proteins in centrosomes. Thus, USP9X plays a role in maintaining centriolar satellite integrity, as important as that of the core satellite scaffold protein PCM1.

The ubiquitin ligase MIB1 binds PCM1 and catalyzes PCM1 polyubiquitylation to promote proteasomal degradation (Wang et al., 2016). Interestingly, MIB1 is also a USP9X-interacting protein (Choe et al., 2007; Mertz et al., 2015). We found that knockdown of MIB1 in USP9X-depleted HeLa cells largely rescues PCM1 protein levels, restores centriolar satellite particles, and restores localization of CEP290 in satellites. The incomplete rescue effect could be due to the low MIB1 knockdown efficiency (~50%), and/or the involvement of other unknown ubiquitin ligases that mediate PCM1 ubiquitylation and degradation. In addition to increasing PCM1 protein levels, knockdown of MIB1 could increase the levels of PLK4 protein, which in turn phosphorylates PCM1 to promote its oligomerization and satellite formation (Hori et al., 2016). Centriolar satellites were proposed as reservoirs of MIB1, which prevent inappropriate localization of MIB1 into centrioles. Otherwise, MIB1 mediates degradation of KIAA0586 and CEP131, which inhibits ciliogenesis (Wang et al., 2016). Our current study found that USP9X counteracts MIB1-mediated ubiquitylation of PCM1 to protect it from proteasomal degradation, which maintains centriolar satellites and thus, constrains MIB1, CEP290 and other proteins in centriolar satellites.

The centriolar satellite, centrosome and primary cilium network is important for human health. Mutations in the growing number of genes encoding proteins of this network are implicated in ciliopathies, including Bardet–Biedl syndrome (*BBS4*), Joubert syndrome (*OFD1*), Meckel Gruber syndrome (*MKS1*, *TMEM216* and *CEP290*), primary microcephaly (MCPH; *WDR62*, *STIL* and *CEP135*) and oral-facial-digital syndrome (*OFD1*) (Faheem et al., 2015; Ko, 2012; Lopes et al., 2011; Pan, 2008; Quinlan et al., 2008; Tollenaere et al., 2015). Primary cilia are signaling hubs that coordinate Hedgehog and GPCR pathways to mediate vertebrate development (Pala et al., 2017; Pedersen et al., 2016; Wheway et al., 2018). Two recent studies identified mutations in *USP9X* that cause female-specific ciliopathy-like syndromes (Homan et al., 2014; Reijnders et al., 2016). Our study adds USP9X to the expanding list of centriolar satellite proteins for which mutations in the encoding genes cause ciliopathies or similar syndromes. It is unknown how *USP9X* mutations cause ciliopathy-like syndromes; we speculate that the loss-of-function mutations of USP9X impair its role in the centriolar satellite, centrosome and primary cilium network, which in turn causes developmental defects and the development of ciliopathy-like syndromes.

MATERIALS AND METHODS

Antibodies and expression constructs

The following antibodies were purchased: anti-CEP290 (A301-659A) and anti-USP9X (A301-351A) (Bethyl Laboratories); anti-CEP290 (SC-390462), anti-USP9X/Y (SC-365353), anti-PCM1 (SC-67204, SC-398365), anti-MIB1 (SC-393811) and anti-ubiquitin (SC-8017) (Santa Cruz Biotechnology); anti-γ-tubulin (T35559) and anti-FLAG (F1804) (Sigma-Aldrich); and anti-CEP131 (25735-I-AP), anti-KIAA0586 (24421-I-AP) and anti-α-tubulin (66031-I-Ig) (Proteintech).

Expression plasmids of USP9X, USP9X deletion mutants, and PCM1 and PCM1 deletion mutants were constructed by PCR, followed by subcloning into the pRK7 vector containing an N-terminal FLAG or Myc tag. All plasmids were validated by DNA sequencing.

Cell culture and transfection

Human embryonic kidney (HEK) 293T, HeLa and HCT116 cells were originally purchased from the American Type Culture Collection, and grown in Dulbecco's modified Eagle medium supplemented with 10% fetal bovine serum (VWR, 89510-186) and 100 µg/ml of penicillin and streptomycin at 37°C with 5% CO_2. Cells were also periodically authenticated and tested for contamination by the Protein Production Core at the University of Colorado Anschutz Medical Campus. The 293T cells were grown to 50–60% confluence and transfected using the standard calcium phosphate precipitation method (Jordan et al., 1996). Typically, 10 µg of each plasmid was used for transfection of cells in a 100-mm dish. Usually, cells were harvested after 48 h transfection. For experiments where indicated, 10 µM MG132 (UBPBio, F1101) was supplemented in medium for 8–16 h before harvesting.

Establishing stable cell lines

A lentivirus-based method was used to generate stable cell lines as described previously (Han et al., 2012). Two different shRNA constructs in pLKO.1 vector targeting human *USP9X* (TRCN0000007361 and TRCN0000-0007364), human *MIB1* (TRCN0000352693 and TRCN0000004554) or human *CEP290* (TRCN000142313 and TRCN000145444), and a control *EGFP* shRNA (SHC005), were purchased from the Functional Genomics Core Facility at the University of Colorado. To stably knock down MIB1 in USP9X knockdown cells, we swapped the puromycin-resistant gene in the *USP9X* shRNA construct (TRCN0000007361) with a neomycin-resistant gene. HeLa cells were infected with *USP9X* shRNA-containing virus and selected with 2 mg/ml neomycin for 2 weeks. The cells were further infected with *MIB1* shRNA-containing virus, and then selected with 2 µg/ml puromycin for at least 5 days, or until all cells in a negative control infection were killed.

Immunoprecipitation and immunoblotting assays

For non-denaturing immunoprecipitation, cells in a 100-mm dish (90% confluence) were harvested and washed with 1× PBS, then lysed with 1.0 ml cold cell lysis buffer (20 mM Tris-HCl, pH 7.6, 150 mM NaCl, 2 mM EDTA, 0.5% Triton X-100, 10% glycerol) with protease inhibitor cocktails (Roche). After clearing lysates by centrifugation, supernatants were incubated with 1 µg of an appropriate antibody or control IgG for 4 h at 4°C, then supplemented with 20 µl protein A beads that were preincubated with 2 mg/ml bovine serum albumin (BSA) to reduce non-specific binding. After overnight rocking, protein A beads were pelleted by centrifugation and washed three times with the cell lysis buffer plus 0.5 M NaCl, unless otherwise specified. Bound proteins were eluted in 50 µl 1× SDS sample buffer. For denaturing immunoprecipitation, cells in a 100-mm dish were lysed in 1 ml cell lysis buffer plus 1% SDS. Cell lysates were collected and then heated at 95°C for 15 min. After centrifugation, 0.3 ml supernatants were diluted with 1.2 ml cell lysis buffer to reduce SDS concentration to 0.2%. The immunoprecipitation assay was performed as described above, except that 5 µg anti-FLAG M2 antibody or mouse IgG was used in each

reaction. Eluates (20 µl) were resolved in SDS-PAGE and transferred to nitrocellulose membranes for immunoblotting assays. Immunoblotting images were captured using a ChemiDoc MP Imaging system (Bio-Rad).

Immunofluorescence staining

Immunofluorescence staining and imaging were performed as described previously (Han et al., 2016). Briefly, cells cultured on glass coverslips were fixed with 100% methanol at −20°C for 10 min and then blocked with blocking buffer (3% BSA in TTBS) for 1 h. Cells were then incubated with an appropriate primary antibody (1:200–1:1000 dilution) in blocking buffer overnight at 4°C, followed by incubation with an anti-mouse or -rabbit IgG (H+L) (Alexa Fluor 488 or 555 conjugated) (Cell Signaling Technology, 4412 and 4409, respectively) for 1 h at room temperature. The coverslip was mounted with the ProLong® Gold Antifade Kit (Thermo Fisher Scientific, P7481) containing the blue fluorescent nuclear counterstain DAPI. Images were captured using a Leica DM 500B fluorescence microscope with a 100× oil immersion objective lens.

Statistical analysis

To quantify PCM1 foci and their colocalization with USP9X or CEP290, at least 100 cells in each of the three different sections of a slide were counted. Data represent the mean±s.d. Statistical analysis was performed using two-tailed unpaired Student's *t*-tests, from which s.d. and *P*-values were calculated. A *P*-value <0.05 was considered statistically significant.

Acknowledgements

We thank Dr Bruce Appel for insightful discussion.

Competing interests

The authors declare no competing or financial interests.

Author contributions

Conceptualization: K.-J.H., C.-W.L.; Methodology: K.-J.H., C.-W.L.; Formal analysis: K.-J.H., Z.W., C.G.P., J.P., K.S., C.-W.L.; Resources: C.-W.L.; Data curation: K.-J.H., Z.W., C.G.P., J.P., K.S., C.-W.L.; Writing - original draft: K.-J.H., C.-W.L.; Writing - review & editing: K.-J.H., Z.W., C.G.P., J.P., K.S., C.-W.L.; Supervision: C.-W.L.; Project administration: C.-W.L.; Funding acquisition: C.-W.L.

Funding

This study was partially supported by the Cancer League of Colorado, the Foundation for the National Institutes of Health [U01CA222958 to C.-W.L.] and the National Institutes of Health [R01GM114260 to J.P. and R01GM099820 to C.G.P.]. The Functional Genomics Core Facility at the University of Colorado Anschutz Medical Campus is partially supported by the Cancer Center, University of Colorado [P30CA046934]. Deposited in PMC for release after 12 months.

Supplementary information

Supplementary information available online at
http://jcs.biologists.org/lookup/doi/10.1242/jcs.221663.supplemental

References

Al-Hakim, A. K., Zagorska, A., Chapman, L., Deak, M., Peggie, M. and Alessi, D. R. (2008). Control of AMPK-related kinases by USP9X and atypical Lys(29)/Lys(33)-linked polyubiquitin chains. *Biochem. J.* **411**, 249-260.

Bärenz, F., Mayilo, D. and Gruss, O. J. (2011). Centriolar satellites: busy orbits around the centrosome. *Eur. J. Cell Biol.* **90**, 983-989.

Chavali, P. L., Putz, M. and Gergely, F. (2014). Small organelle, big responsibility: the role of centrosomes in development and disease. *Philos. Trans. R. Soc. Lond. B Biol. Sci.* **369**, 20130468.

Choe, E.-A., Liao, L., Zhou, J.-Y., Cheng, D., Duong, D. M., Jin, P., Tsai, L.-H. and Peng, J. (2007). Neuronal morphogenesis is regulated by the interplay between cyclin-dependent kinase 5 and the ubiquitin ligase mind bomb 1. *J. Neurosci.* **27**, 9503-9512.

Coene, K. L., Roepman, R., Doherty, D., Afroze, B., Kroes, H. Y., Letteboer, S. J., Ngu, L. H., Budny, B., van Wijk, E., Gorden, N. T. et al. (2009). OFD1 is mutated in X-linked Joubert syndrome and interacts with LCA5-encoded lebercilin. *Am. J. Hum. Genet.* **85**, 465-481.

Conkar, D., Culfa, E., Odabasi, E., Rauniyar, N., Yates, J. R., III and Firat-Karalar, E. N. (2017). The centriolar satellite protein CCDC66 interacts with CEP290 and functions in cilium formation and trafficking. *J. Cell Sci.* **130**, 1450-1462.

Coppieters, F., Lefever, S., Leroy, B. P. and De Baere, E. (2010). CEP290, a gene with many faces: mutation overview and presentation of CEP290base. *Hum. Mutat.* **31**, 1097-1108.

Dammermann, A. and Merdes, A. (2002). Assembly of centrosomal proteins and microtubule organization depends on PCM-1. *J. Cell Biol.* **159**, 255-266.

Das, A., Qian, J. and Tsang, W. Y. (2017). USP9X counteracts differential ubiquitination of NPHP5 by MARCH7 and BBS11 to regulate ciliogenesis. *PLoS Genet.* **13**, e1006791.

Drivas, T. G. and Bennett, J. (2014). CEP290 and the primary cilium. *Adv. Exp. Med. Biol.* **801**, 519-525.

Dupont, S., Mamidi, A., Cordenonsi, M., Montagner, M., Zacchigna, L., Adorno, M., Martello, G., Stinchfield, M. J., Soligo, S., Morsut, L. et al. (2009). FAM/USP9x, a deubiquitinating enzyme essential for TGFbeta signaling, controls Smad4 monoubiquitination. *Cell* **136**, 123-135.

Faheem, M., Naseer, M. I., Rasool, M., Chaudhary, A. G., Kumosani, T. A., Ilyas, A. M., Pushparaj, P., Ahmed, F., Algahtani, H. A., Al-Qahtani, M. H. et al. (2015). Molecular genetics of human primary microcephaly: an overview. *BMC Med. Genomics* **8**, S4.

Ferrante, M. I., Romio, L., Castro, S., Collins, J. E., Goulding, D. A., Stemple, D. L., Woolf, A. S. and Wilson, S. W. (2009). Convergent extension movements and ciliary function are mediated by ofd1, a zebrafish orthologue of the human oral-facial-digital type 1 syndrome gene. *Hum. Mol. Genet.* **18**, 289-303.

Frank, V., den Hollander, A. I., Brüchle, N. O., Zonneveld, M. N., Nürnberg, G., Becker, C., Du Bois, G., Kendziorra, H., Roosing, S., Senderek, J. et al. (2008). Mutations of the CEP290 gene encoding a centrosomal protein cause Meckel-Gruber syndrome. *Hum. Mutat.* **29**, 45-52.

Han, K.-J., Foster, D. G., Zhang, N.-Y., Kanisha, K., Dzieciatkowska, M., Sclafani, R. A., Hansen, K. C., Peng, J. and Liu, C. W. (2012). Ubiquitin-specific protease 9x deubiquitinates and stabilizes the spinal muscular atrophy protein-survival motor neuron. *J. Biol. Chem.* **287**, 43741-43752.

Han, K.-J., Foster, D., Harhaj, E. W., Dzieciatkowska, M., Hansen, K. and Liu, C. W. (2016). Monoubiquitination of survival motor neuron regulates its cellular localization and Cajal body integrity. *Hum. Mol. Genet.* **25**, 1392-1405.

Helou, J., Otto, E. A., Attanasio, M., Allen, S. J., Parisi, M. A., Glass, I., Utsch, B., Hashmi, S., Fazzi, E., Omran, H. et al. (2007). Mutation analysis of NPHP6/CEP290 in patients with Joubert syndrome and Senior-Loken syndrome. *J. Med. Genet.* **44**, 657-663.

Homan, C. C., Kumar, R., Nguyen, L. S., Haan, E., Raymond, F. L., Abidi, F., Raynaud, M., Schwartz, C. E., Wood, S. A., Gecz, J. et al. (2014). Mutations in USP9X are associated with X-linked intellectual disability and disrupt neuronal cell migration and growth. *Am. J. Hum. Genet.* **94**, 470-478.

Hori, A. and Toda, T. (2017). Regulation of centriolar satellite integrity and its physiology. *Cell. Mol. Life Sci.* **74**, 213-229.

Hori, A., Peddie, C. J., Collinson, L. M. and Toda, T. (2015). Centriolar satellite- and hMsd1/SSX2IP-dependent microtubule anchoring is critical for centriole assembly. *Mol. Biol. Cell* **26**, 2005-2019.

Hori, A., Barnouin, K., Snijders, A. P. and Toda, T. (2016). A non-canonical function of Plk4 in centriolar satellite integrity and ciliogenesis through PCM1 phosphorylation. *EMBO Rep.* **17**, 326-337.

Joachim, J., Razi, M., Judith, D., Wirth, M., Calamita, E., Encheva, V., Dynlacht, B. D., Snijders, A. P., O'Reilly, N., Jefferies, H. B. J. et al. (2017). Centriolar satellites control GABARAP ubiquitination and GABARAP-mediated autophagy. *Curr. Biol.* **27**, 2123-2136 e7.

Jordan, M., Schallhorn, A. and Wurm, F. M. (1996). Transfecting mammalian cells: optimization of critical parameters affecting calcium-phosphate precipitate formation. *Nucleic Acids Res.* **24**, 596-601.

Katsanis, N., Lupski, J. R. and Beales, P. L. (2001). Exploring the molecular basis of Bardet-Biedl syndrome. *Hum. Mol. Genet.* **10**, 2293-2299.

Kim, J., Krishnaswami, S. R. and Gleeson, J. G. (2008). CEP290 interacts with the centriolar satellite component PCM-1 and is required for Rab8 localization to the primary cilium. *Hum. Mol. Genet.* **17**, 3796-3805.

Ko, H. W. (2012). The primary cilium as a multiple cellular signaling scaffold in development and disease. *BMB Rep* **45**, 427-432.

Kurtulmus, B., Wang, W., Ruppert, T., Neuner, A., Cerikan, B., Viol, L., Dueñas-Sánchez, R., Gruss, O. J. and Pereira, G. (2016). WDR8 is a centriolar satellite and centriole-associated protein that promotes ciliary vesicle docking during ciliogenesis. *J. Cell Sci.* **129**, 621-636.

Li, X., Song, N., Liu, L., Liu, X., Ding, X., Song, X., Yang, S., Shan, L., Zhou, X., Su, D. et al. (2017). USP9X regulates centrosome duplication and promotes breast carcinogenesis. *Nat. Commun.* **8**, 14866.

Lopes, C. A. M., Prosser, S. L., Romio, L., Hirst, R. A., O'Callaghan, C., Woolf, A. S. and Fry, A. M. (2011). Centriolar satellites are assembly points for proteins implicated in human ciliopathies, including oral-facial-digital syndrome 1. *J. Cell Sci.* **124**, 600-612.

Mertz, J., Tan, H., Pagala, V., Bai, B., Chen, P.-C., Li, Y., Cho, J. H., Shaw, T., Wang, X. and Peng, J. (2015). Sequential elution interactome analysis of the mind bomb 1 ubiquitin ligase reveals a novel role in dendritic spine outgrowth. *Mol. Cell. Proteomics* **14**, 1898-1910.

Murray, R. Z., Jolly, L. A. and Wood, S. A. (2004). The FAM deubiquitylating enzyme localizes to multiple points of protein trafficking in epithelia, where it associates with E-cadherin and beta-catenin. *Mol. Biol. Cell* **15**, 1591-1599.

Murtaza, M., Jolly, L. A., Gecz, J. and Wood, S. A. (2015). La FAM fatale: USP9X in development and disease. *Cell. Mol. Life Sci.* **72**, 2075-2089.

Olsen, J. V., Vermeulen, M., Santamaria, A., Kumar, C., Miller, M. L., Jensen, L. J., Gnad, F., Cox, J., Jensen, T. S., Nigg, E. A. et al. (2010). Quantitative phosphoproteomics reveals widespread full phosphorylation site occupancy during mitosis. *Sci. Signal.* **3**, ra3.

Paemka, L., Mahajan, V. B., Ehaideb, S. N., Skeie, J. M., Tan, M. C., Wu, S., Cox, A. J., Sowers, L. P., Gecz, J., Jolly, L. et al. (2015). Seizures are regulated by ubiquitin-specific peptidase 9 X-linked (USP9X), a de-ubiquitinase. *PLoS Genet.* **11**, e1005022.

Pala, R., Alomari, N. and Nauli, S. M. (2017). Primary cilium-dependent signaling mechanisms. *Int. J. Mol. Sci.* **18**.

Pan, J. (2008). Cilia and ciliopathies: from Chlamydomonas and beyond. *Sci. China C Life Sci.* **51**, 479-486.

Pedersen, L. B., Mogensen, J. B. and Christensen, S. T. (2016). Endocytic control of cellular signaling at the primary cilium. *Trends Biochem. Sci.* **41**, 784-797.

Perrault, I., Delphin, N., Hanein, S., Gerber, S., Dufier, J. L., Roche, O., Defoort-Dhellemmes, S., Dollfus, H., Fazzi, E., Munnich, A. et al. (2007). Spectrum of NPHP6/CEP290 mutations in Leber congenital amaurosis and delineation of the associated phenotype. *Hum. Mutat.* **28**, 416.

Quinlan, R. J., Tobin, J. L. and Beales, P. L. (2008). Modeling ciliopathies: Primary cilia in development and disease. *Curr. Top. Dev. Biol.* **84**, 249-310.

Reijnders, M. R., Zachariadis, V., Latour, B., Jolly, L., Mancini, G. M., Pfundt, R., Wu, K. M., van Ravenswaaij-Arts, C. M., Veenstra-Knol, H. E., Anderlid, B. M. et al. (2016). De Novo loss-of-function mutations in USP9X cause a female-specific recognizable syndrome with developmental delay and congenital malformations. *Am. J. Hum. Genet.* **98**, 373-381.

Santamaria, A., Wang, B., Elowe, S., Malik, R., Zhang, F., Bauer, M., Schmidt, A., Sillje, H. H., Korner, R. and Nigg, E. A. (2011). The Plk1-dependent phosphoproteome of the early mitotic spindle. *Mol. Cell. Proteomics* **10**, M110 004457.

Schwickart, M., Huang, X., Lill, J. R., Liu, J., Ferrando, R., French, D. M., Maecker, H., O'Rourke, K., Bazan, F., Eastham-Anderson, J. et al. (2010). Deubiquitinase USP9X stabilizes MCL1 and promotes tumour cell survival. *Nature* **463**, 103-107.

Shearer, R. F., Frikstad, K.-A. M., McKenna, J., McCloy, R., Deng, N., Burgess, A., Stokke, T., Patzke, S. and Saunders, D. N. (2018). The E3 ubiquitin ligase UBR5 regulates centriolar satellite stability and primary cilia. *Mol. Biol. Cell* **29**, 1542-1554.

Tollenaere, M. A., Mailand, N. and Bekker-Jensen, S. (2015). Centriolar satellites: key mediators of centrosome functions. *Cell. Mol. Life Sci.* **72**, 11-23.

Valente, E. M., Silhavy, J. L., Brancati, F., Barrano, G., Krishnaswami, S. R., Castori, M., Lancaster, M. A., Boltshauser, E., Boccone, L. and Al-Gazali, L. et al. (2006). Mutations in CEP290, which encodes a centrosomal protein, cause pleiotropic forms of Joubert syndrome. *Nat. Genet.* **38**, 623-625.

Villumsen, B. H., Danielsen, J. R., Povlsen, L., Sylvestersen, K. B., Merdes, A., Beli, P., Yang, Y. G., Choudhary, C., Nielsen, M. L., Mailand, N. et al. (2013). A new cellular stress response that triggers centriolar satellite reorganization and ciliogenesis. *EMBO J.* **32**, 3029-3040.

Wang, L., Lee, K., Malonis, R., Sanchez, I. and Dynlacht, B. D. (2016). Tethering of an E3 ligase by PCM1 regulates the abundance of centrosomal KIAA0586/Talpid3 and promotes ciliogenesis. *Elife* **5**, 12950.

Wang, Q., Tang, Y., Xu, Y., Xu, S., Jiang, Y., Dong, Q., Zhou, Y. and Ge, W. (2017). The X-linked deubiquitinase USP9X is an integral component of centrosome. *J. Biol. Chem.* **292**, 12874-12884.

Wheway, G., Nazlamova, L. and Hancock, J. T. (2018). Signaling through the Primary Cilium. *Front. Cell Dev. Biol.* **6**, 8.

Zhang, B., Wang, G., Xu, X., Yang, S., Zhuang, T., Wang, G., Ren, H., Cheng, S. Y., Jiang, Q. and Zhang, C. (2017). DAZ-interacting protein 1 (Dzip1) phosphorylation by polo-like kinase 1 (Plk1) regulates the centriolar satellite localization of the BBSome protein during the cell cycle. *J. Biol. Chem.* **292**, 1351-1360.